



# A study on the convective heating method of cold weather concreting

Uranchimeg Davaasuren<sup>1</sup>, Duinkherjav Yagaanbuyant<sup>1</sup>, Khishgee Radnaabazar<sup>1\*</sup>, Bolormunkh Gantugs<sup>1</sup>

<sup>1</sup> Department of Structural Engineering, School of Civil Engineering and Architecture, Mongolian University of Science and Technology, Ulaanbaatar, Mongolia

\* Correspondence author. Email: [khishgee\\_radnaa@must.edu.mn](mailto:khishgee_radnaa@must.edu.mn)

## ABSTRACT

In Mongolia, construction work in the coldest months of the year decreases dramatically due to a lack of reliable technology methods for cold weather concreting. Last 10 to 15 years, the convective heating method has started to be dominantly used in cold weather concreting in the country but comprehensive study on this method still lacks. The convective heating environment that is close to the actual construction site was created to cure concrete column specimens and their internal temperature distribution, compressive strength, and pore structure developments were studied. The importance of air circulation inside the heated enclosure is common knowledge, but due to its difficulty it is mostly omitted in the current practice leading differential temperature fields in vertical structures like columns and walls, this issue was studied. The results of the temperature study at the contact surface between old and new concrete in cold weather were discussed.

**Keywords:** Cold weather concreting, convective heating, concrete column structure, temperature field, compressive strength, porosity.

## 1. INTRODUCTION

In cold weather concreting, protection & curing method selection is mostly affected by ambient air temperature and geometry of a structure. Mongolian Building Code BNbD 52-02-02 specifies to use of an additional heat supply to the concrete structure that is going to be cast when the ambient air temperature is below  $-25^{\circ}\text{C}$  and the structure's surface modulus is higher than  $-3\text{m}^{-1}$  to protect it against frost-related damages [1-3]. The surface modulus is the ratio of the total cooling surface area to the total volume of a structure. The currently used protection and curing methods in this condition are electrode heating, heating formworks, heated enclosures, induction methods, etc. [2]. Internationally a method that builds a temporary enclosure around the casting concrete structure to heat its surrounding air is called 'the heated enclosure method', but lately in Russian literature, this method is called as 'convective heating method' as its primary heat transfer mode is air convection from surrounding warm air to the surface of the formwork of the structures [2]. Mongolian concrete literature mostly takes after Russian practice in cold weather concreting and now terminology of

convective heating is started to be used in the industry, therefore it is used in this paper.

In the coldest months of the Mongolian winter, the ambient air temperature drops below  $-25^{\circ}\text{C}$  even in the daytime which leads to a significant drop in construction work amount. The increased cost of construction work in this weather is the primary reason. Before the 2000s, the dominant curing method in cold weather concreting was electrode heating, but the convective heating method has become a trend in the last 10 to 15 years. A combustion heater is used to heat the inside air of the temporarily built enclosure around the concrete structures and due to this, the cost of this method is relatively high. In this method, the importance of air circulation inside the enclosure is common knowledge, but due to its difficulty, it is mostly omitted in the current construction practice in Mongolia. The authors previously did on-site temperature measurements of RC columns on the 6<sup>th</sup> floor of a 10-story RC frame office building in January 2020. The concrete was cast and cured by the convective heating method. From this study, it was observed that the internal temperatures of columns differed vastly along their heights ranging from  $5^{\circ}\text{C}$  at the bottom to  $40^{\circ}\text{C}$  at the top

[4]. This differential temperature condition resulted not only from the lack of air circulation inside the enclosure but also from the lower temperature of the contact areas of the fresh concrete at the joint.

In the cold weather after the initial few days of accelerated curing the structures kept frost before the next floor's casting. Heating is applied to the frozen structures, formwork, and reinforcements to prepare the contact surfaces of the fresh concrete. Mongolian Building Code BNbD 52-02-05 requires preparing the contact surfaces before fresh concrete pouring to avoid any freezing and if thermal calculation shows any probability of freezing then take heating actions. It also stipulates that when the structure has densely packed reinforcements or large-size embedded items in the ambient temperature below  $-10^{\circ}\text{C}$  then reinforcements and embedded items must have a temperature above  $0^{\circ}\text{C}$  at the time of fresh concrete pouring [1]. Following these requirements, it became a usual practice to accept lower temperatures just above  $0^{\circ}\text{C}$  for contact surfaces of fresh concrete in the industry, and it contributes to the above-mentioned lower curing temperatures at the bottom parts of the newly cast vertical structures like columns and walls.

The initial temperature of the concrete has a significant effect on the cement hydration. In most literature, structural elements of thicker sections or mass concrete are studied in which the internal temperature can reach a significant level. In those structures, the lower placing temperature reduces the risk of early-age thermal cracking [5-8]. Xie et.al studied the initial temperature effect on the hydration characteristics and pore structure of cement systems and reported that a  $10^{\circ}\text{C}$  increase in the initial temperature of OPC increases the maximum temperature by around  $16^{\circ}\text{C}$  [8]. Wang et al studied the effect of different initial temperatures on the rate and the total amount of hydration and also showed the direct relationship between the initial concrete temperature and the maximum temperature rise [6]. Even though temperature variations and resulting volume changes that lead to thermal stresses including the effect of the initial temperature in mass concrete are studied extensively there is negligible work involved with non-mass concrete that is cured in cold weather. In cold weather, lower initial concrete temperature leads to slower strength gain thus it is common practice to order warmer concrete mix from the supplier to elevate the initial placement temperature. Even though the concrete mix temperature is high, the temperature of its contact surface is low then this might lead to inconsistent setting, rapid moisture loss, and plastic shrinkage cracking. Therefore, ACI 306R-16 recommends limiting contact surface temperature to be no more than  $5^{\circ}\text{C}$  greater or  $8^{\circ}\text{C}$  less than that of the concrete to avoid these problems [9]. Mongolian Building Code BNbD 52-02-05 doesn't have such limiting provisions.

In cold weather, most protection and curing methods have an accelerating effect on cement hydration resulting in elevated internal temperature in concrete structures at early ages. Study findings show that concrete subjected to higher curing temperature undergoes accelerated hydration resulting in lower long-term strength and greater porosity [10-15]. Galluchi, Zhang, and Scrivener (2013) studied the temperature effect on concrete properties and microstructure by isothermal curing of cement paste samples in  $5^{\circ}\text{C}$ ,  $20^{\circ}\text{C}$ ,  $40^{\circ}\text{C}$ , and  $60^{\circ}\text{C}$  for one year. The results showed that the increased temperature during curing leads to the microstructure of the cement paste that is much coarser and porous and to a lower final strength [13].

In this paper, concrete columns were selected as the study objects, and the effect of the contact surface temperatures on the further temperature evolution of newly-cast concrete was studied under the use of the convective heating method. At the age of 365 days, concrete compressive strength and pore structure were studied.

## 2. EXPERIMENTAL PROCEDURE

### 2.1 Outline of the experiment settings

To simulate in-situ curing conditions, a temporary enclosure with the size of  $11,5 \times 6,0 \times 3,4$  m was built next to the existing laboratory building using its outer wall. The layout and general overview of the enclosure are shown in Fig. 1.

Nine (9) short concrete column specimens (S3-4, S6-12) of the size of  $500 \text{ mm} \times 500 \text{ mm} \times 1200 \text{ mm}$  (width  $\times$  height  $\times$  length), and one (1) long concrete column specimen (S2) of the size  $500 \text{ mm} \times 500 \text{ mm} \times 3000 \text{ mm}$  were cast for the testing. One (1) control short concrete column specimen (S5) of the same size of  $500 \text{ mm} \times 500 \text{ mm} \times 1200 \text{ mm}$  was cast inside the laboratory. A diesel air heater was used to heat the enclosure's interior air.

All 11 concrete column specimens were cast in two parts that have different ages. For the short columns, it aimed to test the different contact surface temperature effects on the temperature distribution of a newly-cast concrete which is the upper part. For the long column, a temperature variation along its length was tested. Even though for the long column, a contact surface temperature wasn't a concern, its base was done in the same way with short column specimens.

At first, 11 column bases of the size of  $500 \text{ mm} \times 500 \text{ mm} \times 600 \text{ mm}$  were cast inside the laboratory and cured at room air temperature for 7 days. In the next step, for 9 short columns that would be cured in the enclosure, their bases were exposed to three different pre-conditions before new concrete was cast and curing started. These three conditions were (1) bases of specimens S3, S4, and S6 were taken directly from laboratory conditions to the

enclosure to cast new concrete; (2) bases of specimens S7, S8, and S9 were frozen outside for 36 hrs prior to the new concrete casting; and (3) bases of specimens S7, S8, and S9 were frozen for 24 hrs and kept back into room condition for 12 hrs prior to the new concrete cast.

## 2.2. Materials

Grade B25 (M350) concrete, with accelerating and superplasticizer admixtures, was used in the test. The concrete slump was 140 mm.

The concrete compressive strength of column specimens was tested at the age of 4 days when curing stopped by ultrasound testing equipment and at the age of 365 days by testing of 100 mm × 200 mm cylindrical cores directly taken from specimens under laboratory compression testing machine.

## 2.3. Temperature measurements

K-type thermocouples were used in temperature measurements and data were recorded by data loggers every half-hour. Each short column temperatures were measured by a total of 4 thermocouples that were installed in two sections. Two sections were 50 mm to each side of the contact surface. In each section, two thermocouples were placed at the center of the section and at 50 mm from the edge to measure the temperature. Each thermocouple had a label that consisted of the specimen number and its location number. In Fig 2a, all short columns' thermocouple locations and labels are shown.

For the 3 m long column, 11 thermocouples were installed in 4 sections as shown in Fig. 2 b. The lowest section is 550 mm above floor level and temperature measurements were taken at the center and at the edge, the same with short columns. The second from the bottom section is 650 mm, the third section is 1800 mm and the top section is 2950 mm above the floor levels respectively as shown in Fig 2 b. The upper three sections had three points for the temperature measurements, one at the center and two at the edges. Each thermocouple had a label and in Fig 2 and 3 all labels of them are shown.

The initial temperature of the concrete mixture was 5°C.

## 2.4. Mercury Intrusion Porosimetry

Mercury Intrusion Porosimetry test was conducted using AutoPoreV9620 made by Micrometrics Instrument Corporation to characterize the pore structure of concrete samples. At the age of 365 days, a total of three concrete cylinder cores of 100 mm × 200 mm were prepared: two from the upper part of specimen S2, and one from the upper part of control specimen S5. For each sample, a disk with a thickness of about 6 mm was obtained from the center using a water-cooled cutter.

The concrete disks were then immersed in pure acetone to cease the cement hydration. Small pieces of concrete with a volume of approximately 5 mm × 5 mm × 5 mm without aggregate were obtained from the concrete disk and vacuum dried. Maximum pressure of 60 000 psi was used.

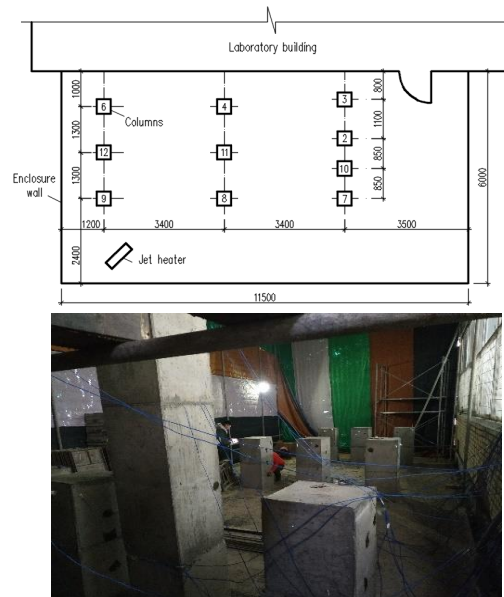


Figure 1 Enclosure layout plan and general view

## 3. RESULTS AND DISCUSSIONS

### 3.1. Concrete temperature evolution

For a total of 84 hrs concrete column specimens were heated and during the last 4 hrs heating rate was decreased gradually by a rate of around 2°C/hr. In Fig. 3a the enclosure interior and ambient air temperatures' history was shown. The lowest ambient air temperature was -17.6°C and the highest inside enclosure temperature was 31.4°C.

In Fig. 3b temperature history of short column specimens S3, S4, and S6 is shown; the bases of these specimens were taken directly from the laboratory to the enclosure, and new concrete was cast. The initial concrete temperature of the curing was 6°C-7°C for these specimens. In Fig. 3c, temperatures of newly cast concrete parts of specimens were shown separately and it can be seen that the maximum internal temperature was in the range of 18,2°C-18,9°C and it happened at 22 hrs from the start of curing. In Fig. 3d, temperatures measured in the bases of these specimens were shown. For S3 and S4, the maximum internal temperature was in the range of 15,4°C-15,5°C which happened at 25 hrs from the start of curing, but for S6 it was 13,8°C. The age difference between the base and the upper newly cast part

is 7 days and hydration heat release was expected only from the upper part's newly cast concrete, not from the base. The difference between the maximum temperatures of the two parts was around  $3.5^{\circ}\text{C}$  and the time difference between these temperature peaks was 3 hrs. Considering the short distance of 100 mm between the two sections where thermocouples were located, it was concluded that the delayed time of temperature peaks in the base was caused by the thermal conductivity. The maximum temperature difference in the section was  $2.8^{\circ}\text{C}$ .

In Fig. 4 temperature history of S7, S8, and S9, which bases were frozen in the outside air for 36 hrs prior to the new concrete casting was shown. The initial concrete temperatures of the curing were in the range of  $0.3^{\circ}\text{C}$ - $0.7^{\circ}\text{C}$  for S7 and S8 while it was  $3.4$ - $6.1^{\circ}\text{C}$  for S9. The reason for the higher initial temperature for S9 is that the specimen's location was the closest to the heater and the following temperatures of this specimen were a little higher too. The maximum temperatures of newly cast concrete parts of S7 and S8 were in the range of  $16.2$ - $17.7^{\circ}\text{C}$  at 23-24 hrs. For S9 it was  $19.3^{\circ}\text{C}$  and it occurred 40 hrs after the start of the curing. The maximum temperature difference in the section was  $5.9^{\circ}\text{C}$ . The maximum difference between the highest temperatures of the two parts was  $3.9^{\circ}\text{C}$  and the time difference between these temperature peaks was 5 hrs.

In Fig. 5 temperature history of S10, S11, and S12, which bases were frozen for 24 hrs and kept back into room condition for 12 hrs prior to the new concrete cast is shown. The initial concrete temperatures of the curing were in the range of  $0.8^{\circ}\text{C}$ - $6.2^{\circ}\text{C}$ . The maximum temperature of newly cast concrete was  $18^{\circ}\text{C}$  at 22 hrs. It is observed that the temperature fluctuation of these specimens was higher than that of S3, S4, and S6 and lower than that of S7, S8, and S9. The maximum temperature difference in the section was  $4.5^{\circ}\text{C}$ .

From temperature histories shown in Fig. 3-5, it is observed that temperature differences in the sections were relatively low differing from the expectations. The highest difference was  $5.9^{\circ}\text{C}$ . A curing condition inside the enclosure was created rather favorable for the internal temperature field developments of the columns. This maximum temperature difference of  $5.9^{\circ}\text{C}$  in the section will not cause any adverse impact on the structure such as a risk of thermal cracking [5-7].

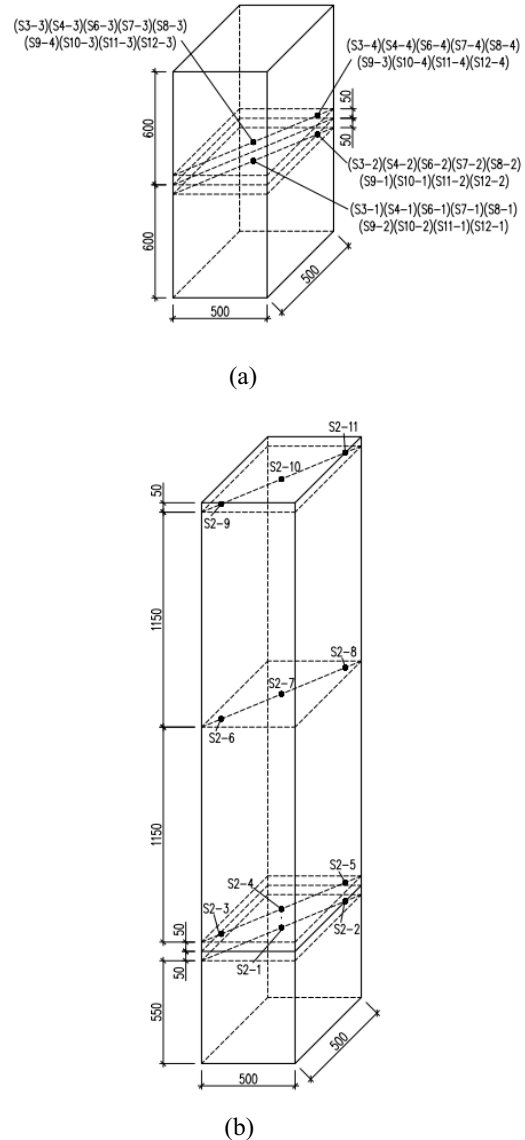
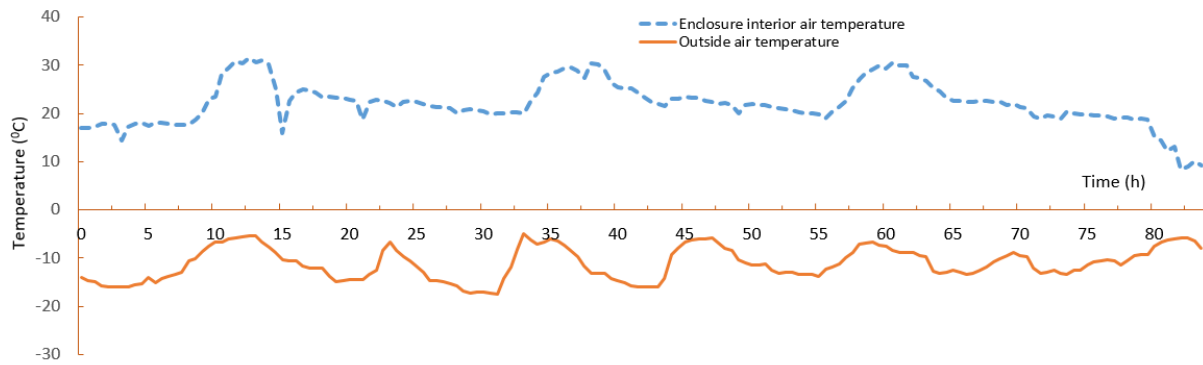
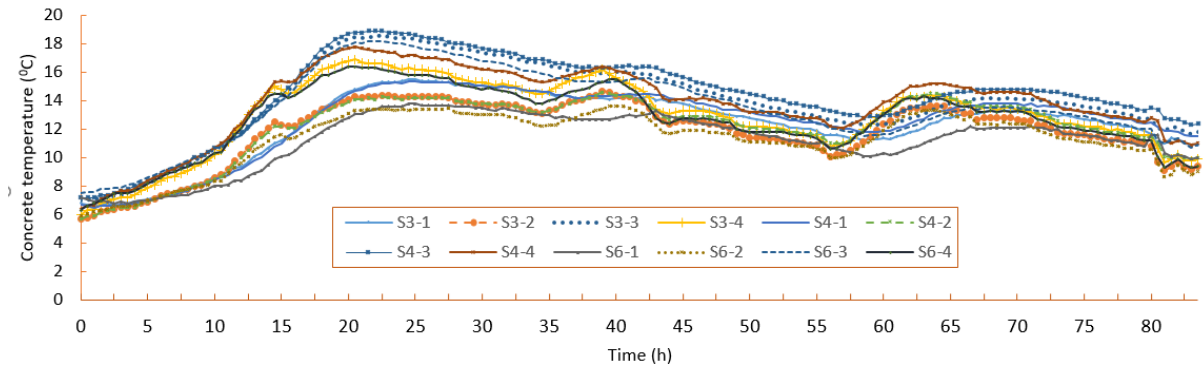


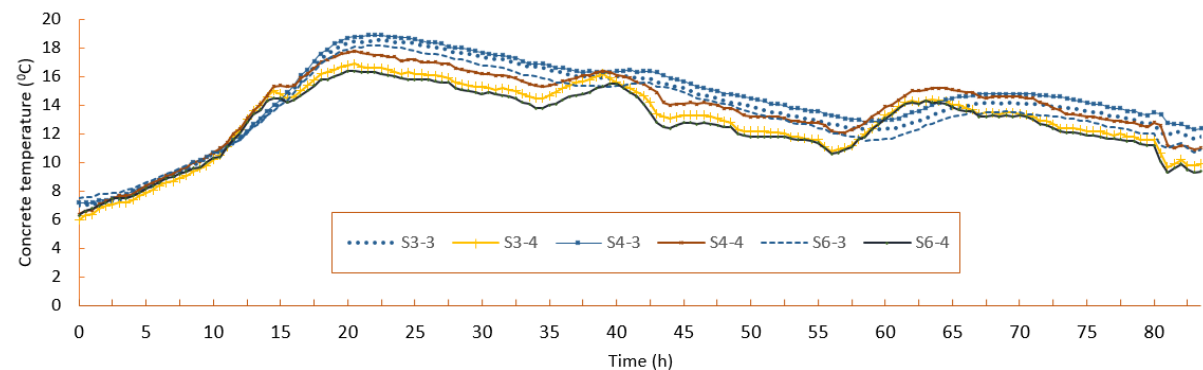
**Figure 2** Concrete specimen geometry and thermocouple locations (a) short columns, (b) long column



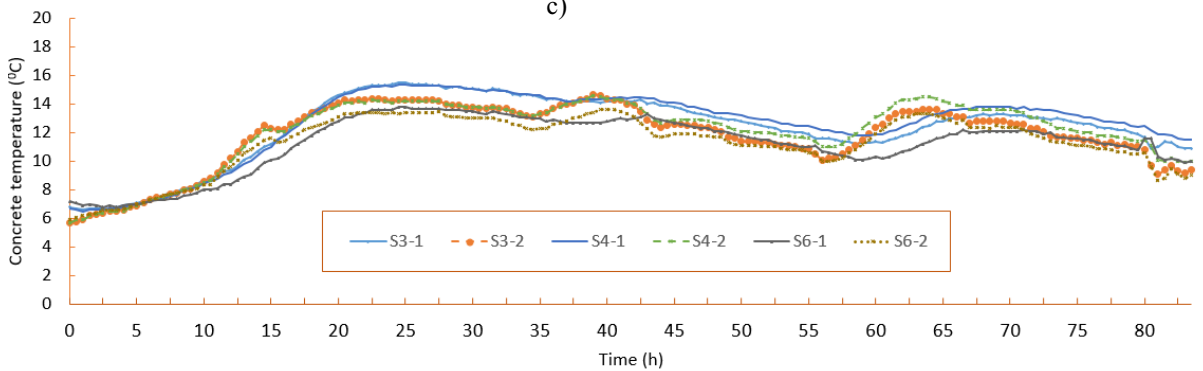
a)



b)



c)



d)

**Figure 3** a) Inside the enclosure and ambient air temperature history; b) S3, S4, S6 specimen internal temperature history; c) S3, S4, S6- upper or newly cast concrete temperatures; d) S3, S4, S6- lower or old concrete temperatures.

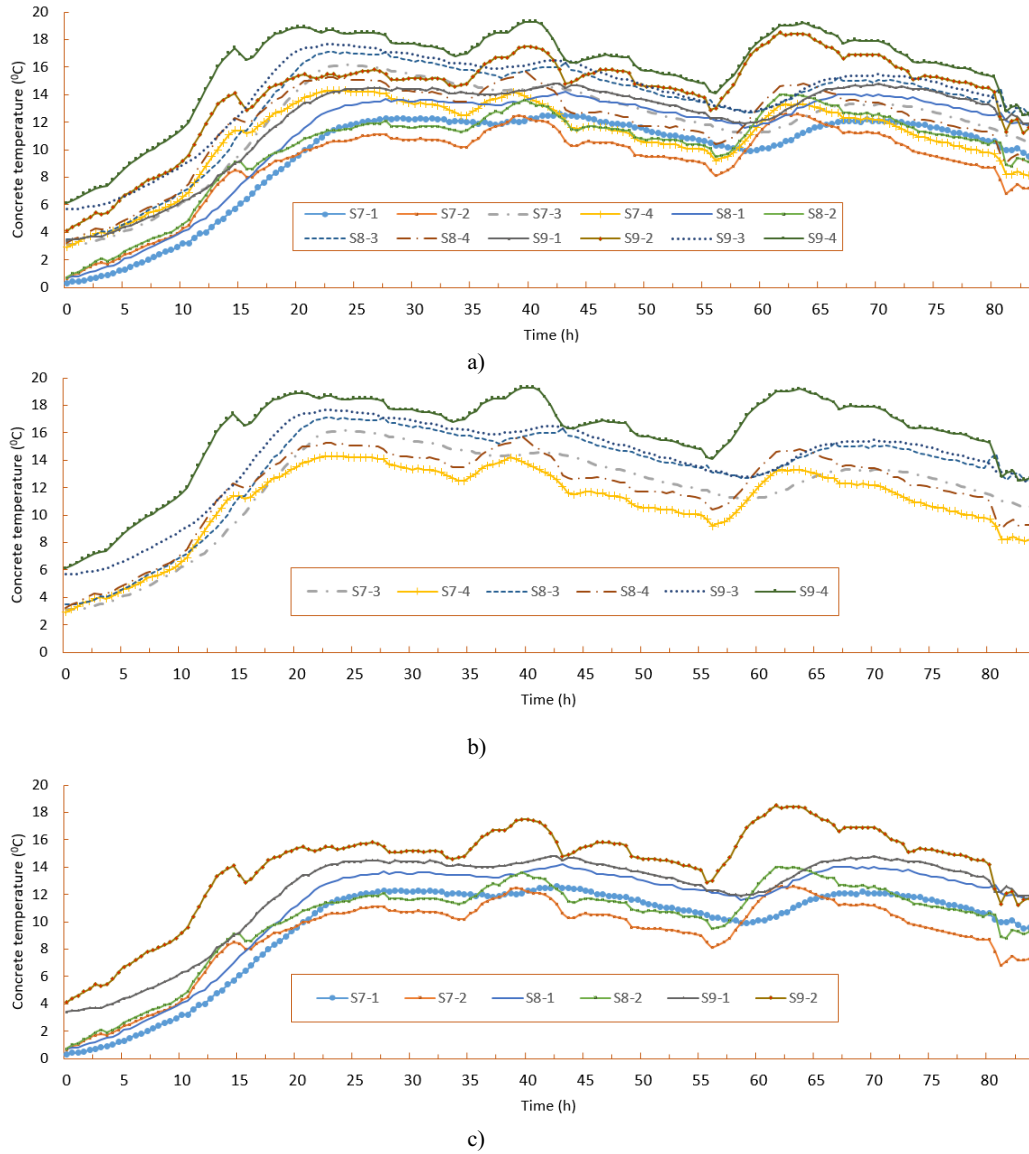


**Figure 4** a) S7, S8, S9 specimen temperature history; b) S7, S8, S9 -upper or newly cast concrete temperatures; c) S7, S8, S9 - lower or old concrete temperatures.

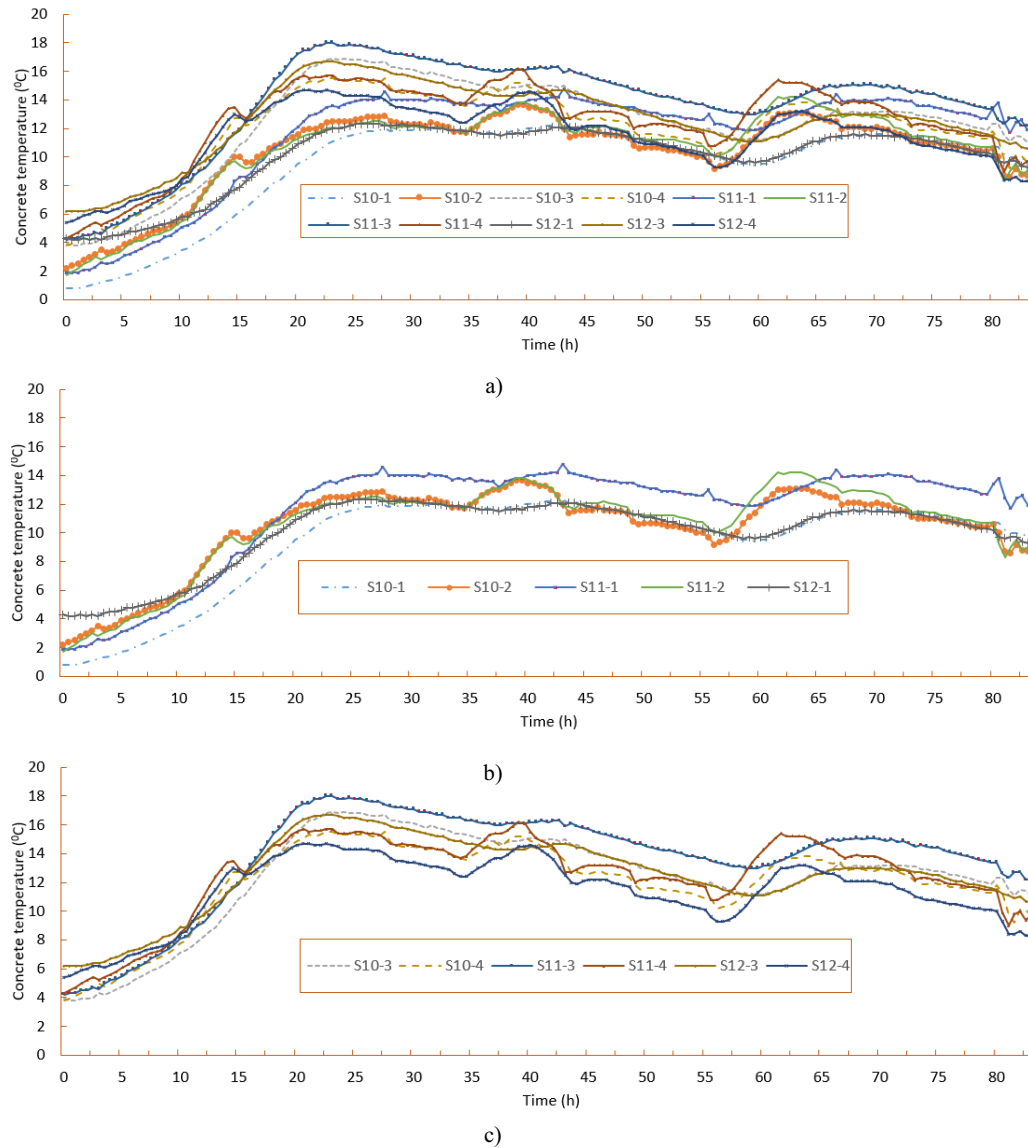


**Figure 5** a) S10, S11, S12 specimen temperature history; b) S10, S11, S12 -upper or newly cast concrete temperatures; c) S10, S11, S12 9-lower or old concrete temperatures.

As mentioned before, the initial concrete temperatures at the start of the curing were 5.7°C to 7.2°C for specimens taken directly from the laboratory, 0.3°C to 6.1°C for specimens frozen outside 36 hrs before the new concrete casting and 0.8°C to 6.2°C for specimens that were frozen for 24 hrs and kept in room condition for 12 hrs. Initial temperatures of specimens located near jet heater had high values, especially for the last two exposure conditions. Even though the initial temperatures differed depending on the exposure conditions, the maximum curing temperatures reached were in the range of 18°C -19°C for all short concrete

column specimens. The direct relationship between the initial and the maximum curing temperature [6, 8] wasn't observed in our study.

Internal temperature variation along the length of the 3 m long column specimen (S2) was measured at 11 locations. Temperature history is shown in Fig. 6. It is observed from the temperature graph that curves are divided visibly into two bands. The lower band consists of the temperature curves measured around the contact surface of 600 mm height of the column and it has the same pattern as the short column internal temperature



curve. The maximum temperature of 18.7°C occurred at 21 hrs after casting and the initial temperature was 7.1°C. The upper band consisted of temperature curves that belong to 1800 mm and 2950 mm heights of the column. The maximum temperature of 30.1°C belongs to the 1800 mm level at 22 hrs. The graph shows that the temperature differs along the length significantly and it indicates a lack of air circulation inside the enclosure.

### 3.2. Concrete compressive strength development

In Fig. 7, concrete compressive strength results at the age of 4 days (at the end of curing) and 365 days are compared respectively among short column specimens S3, S5, S7, and S10. The compressive strength results of only newly cast upper parts' concrete are shown. The compressive strengths at 365 days of S3, S5, S7 and S10 were 43.23MPa, 40.20 MPa, 37.30MPa, and 43.77 MPa respectively. S7 has the lowest value and it is 7.2% lower than the control specimen and about 15% lower than the other two higher strengths. Even though S7 is the specimen whose base was frozen in the outside air for 36 hrs prior to the new concrete casting, its upper new concrete temperature history wasn't low to be noticed.

The laboratory control cubes of 150 mm × 150 mm × 150 mm were cured in the standard laboratory conditions of 28 days in the water at room temperature and during all the remaining time kept at room air. The average value of three cubes is 23 MPa at 4 days, 30.1 MPa at 28 days, and 40.3 MPa at 180 days.

In Fig. 8, the 3 m long column's compressive strength test results are shown. The temperature graphs of this column specimen in Fig. 6 showed distinct differing curves depending on the floor height levels but at 365 days their compressive strength values didn't show any significant difference.

### 3.3. Pore structure

To test the effect of the different curing conditions on the concrete microstructure, two samples from long column S2 and one sample from control specimen S5 were tested by the mercury intrusion porosimetry and results are shown in Fig. 9 and Table 1. Two samples of S2 were taken from the upper new concrete at levels 1200 mm and 2400 mm. A sample from control specimen S5 was taken from the upper new concrete too. All three samples have the age of 365 days. From the cumulative intrusion curves of the three samples that are shown in Fig. 9, the curves of two samples of S2 have similar patterns having coarser pores compared with S5. As given in Table 1, S5's average pore size is 0.0134 μm and it is lower than the other two values of S2. It shows that S5 has finer pores. The control specimen S5 was cured in laboratory air conditions a whole year; and during the

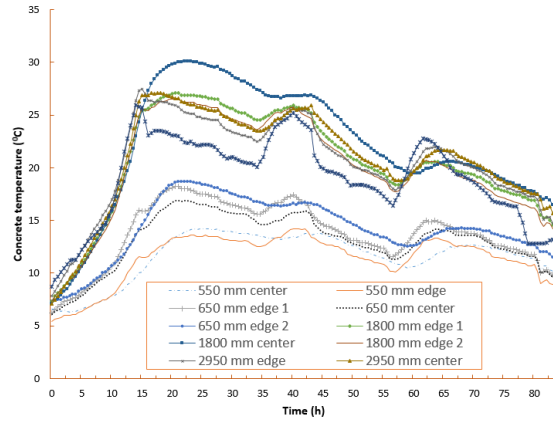


Figure 6 3 m long column S2's concrete temperature history

first 4 days, its highest temperature was 22°C, while the room temperature was around 15°C. If the temperature history of S5 is compared with S2's temperature history then it is between the temperatures curves of the levels of 600 mm and 1800 mm. Therefore, its pore structure cannot be directly related to the internal temperature history of the curing period, but there is a possibility that the frozen state of specimens after the first 4 days of curing might have an effect on this. Choi et al studied the concrete whose compressive strength exceeded 5 MPa exposed to freezing at -20°C for 24 hrs against non-frozen concrete. The compressive strength values of frozen concrete and non-frozen concrete were approximately the same, whereas the frost resistance of frozen concrete was considerably lower than that of non-frozen concrete [16]. The other possible reason of these coarsening was an exposure to the multiple freeze-thaw cycles during the year, but this wasn't supported by the strength test results.

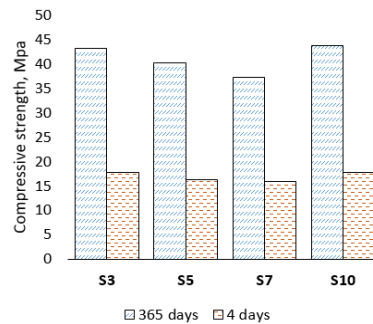
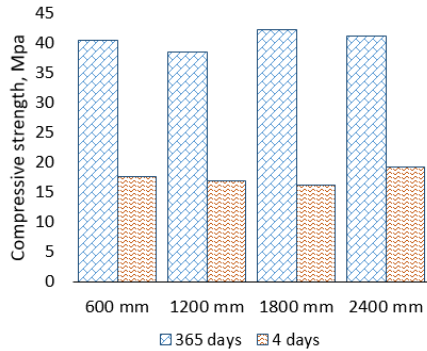
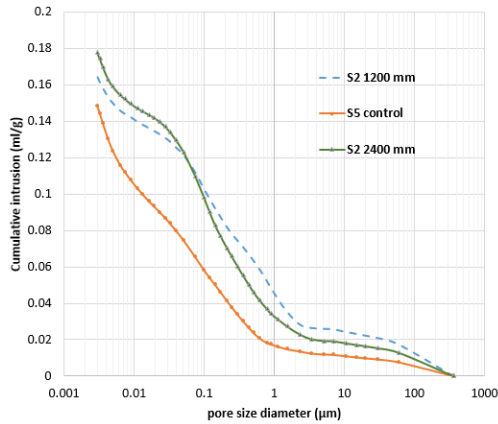


Figure 7 Concrete compressive strength of short column specimens





**Figure 8** Long column concrete compressive strength long its height



**Figure 9** Effect of curing condition on the pore structure of concrete at an age of 365 days

**Table 1.** Parameters of the pore structure testing

Sample ID	Total pore volume (ml/g)	Total pore area (m <sup>2</sup> /g)	Porosity (%)	Average pore size (μm)
S2 newly cast part	0.0806	13.0	16.6	0.0247
S2 base	0.0881	16.2	17.8	0.0217
S5 control	0.0707	21.1	14.8	0.0134

#### 4. CONCLUSIONS

In this study, short and long concrete column specimens cured by the convective heating method in cold weather were studied in terms of their internal temperature distribution, compressive strength, and pore

structure development. The following conclusions were drawn from the study.

1. Even though the initial concrete temperatures at the start of the curing differed depending on the exposure conditions, the maximum curing temperatures actually reached were in the same range for all short concrete column specimens. The previous findings of the direct relationship between the initial and the maximum curing temperature in mass concrete wasn't observed for these specimens.
2. The temperature differences in the sections were relatively low, the highest value was 5.9°C for short columns and it shows that temperature fields in the section are relatively uniform without any risk of thermal cracking in the section.
3. Due to the lack of air circulation inside the enclosure, the temperature fields along the length of the column varied significantly. But the resulting compressive strengths at the age of 365 days were rather consistent without regard to the temperature differential.
4. MIP test results of the 3 m long column specimen showed a coarser pore structure than that of the control specimen.

#### AUTHORS' CONTRIBUTIONS

Uranchimeg Davaasuren: conceptualization, methodology, investigation, experiment, data analysis, writing. Yagaanbuaynt Duinkherjav: conceptualization, project administration, funding acquisition, review. Khishgee Radnaabazar: conceptualization, methodology, supervision, data analysis, validation, review, editing. Bolormunkh Gantugs: experiment, data collection.

#### ACKNOWLEDGMENTS

This study was financially supported by the Mongolian Foundation of Science and Technology (Contract No. Shu/Ud-2020/03).

#### REFERENCES

- [1] BNbD 52-02-05 Cast in place concrete and reinforced concrete structures, Ministry of Construction and Urban Development of Mongolia, 2005.
- [2] B. A. Krylov, S. A. Ambartsumyan, A. I. Zvezdova, Guidelines of cast in place concrete heating, research institute of concrete and reinforced concrete, NIIZHB, M, 2005, NIJB, M, 2005 [In Russian].
- [3] B. Narantogtokh, T. Nishiwaki, D. Pushpalal, Current issues and questionnaire survey of cold weather concreting in Mongolia, Buildings, 12,

- 1262 (2022), <https://doi.org/10.3390/buildings12081262>
- [4] R. Khishgee, Ya. Duinkherjav, D. Uranchimeg, Kh. Naranbayar, Temperature requirements for reinforced concrete structures cast in cold weather, *MUST Scientific Journal* 22(14)-302, (2022) [in Mongolian]
- [5] M. Al-Gburi., Restraint effects in early age concrete structures, Dept. of Civil, Environmental and Natural Resources Engineering, Luleå University of Technology, Doctoral Thesis, Sep. 2015.
- [6] XF. Wang, Q. Chen, J. Tao, R. Han, XB. Ding, F. Xing, N. Han, Concrete thermal stress analysis during tunnel construction, *Adv in Mech Eng*, 11-6 (2019), pp. 1–15, <https://doi.org/10.1177/1687814019852232>
- [7] B. Klemczak, A. Knoppik-Wróbel, Analysis of Early-Age Thermal and shrinkage stresses in reinforced concrete walls, *ACI Structural Journal*, 111- 2, (2014), pp 313-322. <https://doi.org/10.14359/51686523>
- [8] Y. Xie, Ch. Qian, Y. Xu, M. Wei, W. Du, Hydration Heat and microstructure of scm-blended cement under the semi-adiabatic conditions: effect of initial temperatures, *construction and building materials*, 356 (2022) 129329, <https://doi.org/10.1016/j.conbuildmat.2022.129329>.
- [9] ACI 306R-16 Guide to Cold Weather Concreting. american concrete institute: farmington hills, MI, America, 2016,
- [10] S. Yousuf, P. Shafiqh, Z. Ibrahim, H. Hashim, M. Panjehpour, Crossover effect in cement based materials: a review, *Appl. Sci.*, 9 (2019), 2776; <https://doi.org/10.3390/app9142776>.
- [11] H.Jin, Late-age properties of concrete with different binders cured under 45°C at early ages, *Advances in Materials Science and Engineering*, (2017), <https://doi.org/10.1155/2017/8425718>.
- [12] T.A. Do, D. Verdugo, M. Tia, T. T. Hoang, Effect of volume-to-surface area ratio and heat of hydration on early-age thermal behavior of precast concrete segmental box girders, *Case Studies in Thermal Engineering* 28 (2021), <https://doi.org/10.1016/j.csite.2021.101448>
- [13] E. Gallucci, X. Zhang, K.L. Scrivener, Effect of temperature on the microstructure of calcium silicate hydrate (C-S-H), *Cement and Concrete Research* 53, (2013), pp.185–195. <https://doi.org/10.1016/j.cemconres.2013.06.008>
- [14] S. Care, Effect of temperature on porosity and on chloride diffusion in cement pastes, *Construction and Building Materials*, 22 (2008), pp. 1560–1573, <https://doi.org/10.1016/j.conbuildmat.2007.03.018>.
- [15] F. Yousuf, W. Xiaosheng, Early strength development and hydration of cement pastes at different temperatures or with superplasticiser characterised by electrical resistivity, *Case Studies in Construction Materials*, 16 (2022) <https://doi.org/10.1016/j.cscm.2022.e00911>
- [16] H. Choi, W. Zhang, Y. Hama, Method for determining early-age frost damage of concrete by using air-permeability index and influence of early-age frost damage on concrete durability. *Constr. Build. Mater*, 153, (2017), pp. 630–639. <https://doi.org/10.1016/j.conbuildmat.2017.07.140>

**Open Access** This chapter is licensed under the terms of the Creative Commons Attribution-NonCommercial 4.0 International License (<http://creativecommons.org/licenses/by-nc/4.0/>), which permits any noncommercial use, sharing, adaptation, distribution and reproduction in any medium or format, as long as you give appropriate credit to the original author(s) and the source, provide a link to the Creative Commons license and indicate if changes were made.

The images or other third party material in this chapter are included in the chapter's Creative Commons license, unless indicated otherwise in a credit line to the material. If material is not included in the chapter's Creative Commons license and your intended use is not permitted by statutory regulation or exceeds the permitted use, you will need to obtain permission directly from the copyright holder.

